Supplementary material for the paper *Transitional flow of a rarefied gas over a spinning sphere*

ALEXEY N. VOLKOV[1]

[1]Department of Materials Science and Engineering, University of Virginia, 395 McCormick Road, Charlottesville, VA 22904-4745, USA

SM 1. Numerical approach for simulation of transitional flows over a spinning sphere

In the present paper, transitional flows over a spinning sphere are simulated by the direct simulation Monte Carlo (DSMC) method that is known to be a numerical technique for solving kinetic problems based on the Boltzmann equation (Nanbu 1980; Ivanov & Rogasinsky 1988; Wagner 1992; Ivanov & Gimelshein 1998; Cercignani 2000). The 'No Time Counter' (NTC) approach (Bird 1994) is used for the collision sampling. Pseudo-random numbers are generated with an algorithm proposed by Matsumoto & Nishimura (1998).

The sphere is placed in the centre of the rectangular computational domain (Figure SM 1) of size $L \times H \times H$. The inflow of gas molecules is described by the Maxwellian distribution given by (2.4) and imposed on all external boundaries of the computational domain. Simulated molecules, leaving the computational domain, are excluded from the consideration. Such conditions on the external boundaries are suitable for supersonic flow. In order to apply these conditions in subsonic flow, the external boundaries must be placed far enough from the sphere surface. A special study was conducted in order to assess the effect of these boundary conditions in subsonic flows and reasonably choose positions of the external boundaries. A part of simulations at $\Theta = 90^\circ$ was performed in a half of the entire computational domain shown in figure SM 1, which corresponds to $y \geqslant 0$, with the symmetry boundary conditions imposed in the plane of symmetry at $y = 0$.

A computational grid of uniform cubic cells with the cell size Δ is introduced in the computational domain for the collision sampling in the DSMC method. Close to the sphere surface, cells are cut by the surface and volumes of such cells are calculated by means of a special algorithm. The number of simulated molecules is controlled by the average number of simulated molecules N_{cell} in a cell with volume Δ^3 placed in the free stream, so the statistical weight of every simulated molecule is equal to $n_\infty \Delta^3 / N_{cell}$. Simulations of subsonic flows at $Kn = 0.01$ were performed on non-homogeneous Cartesian meshes with variable cell size.

A simulation for given Ma, Kn, W, T_s/T_∞, Θ, and α_τ starts from the Maxwellian distribution given by (2.4) in the entire computational domain. Then the transient is simulated during $\bar{N}_{est}$ time steps, until a quasi-steady-state flow is established. During the next $\bar{N}_{sample}$ time steps, parameters of simulated molecules are accumulated for the subsequent computation of fields of macroscopic gas parameters as well as the aerodynamic force $\boldsymbol{F}$, torque $\boldsymbol{T}$, and heat flux Q exerted on the sphere. Every time step has duration Δt.

Most calculations were conducted with a parallel computer code based on the Message

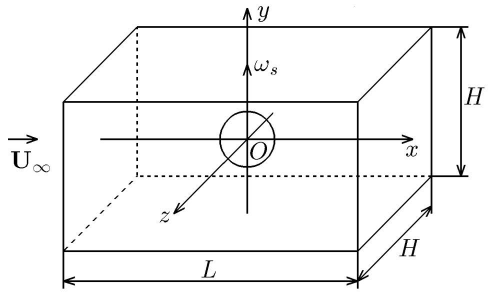

FIGURE SM 1. Sketch of the rectangular computational domain used in the DSMC simulations of transitional flow over a spinning sphere.

Ma	Kn	W	L/R	H/R	Δ/R	$\Delta t/\tau_\infty$	N_{cell}	$\bar{N}_{sample}$
$0.03-1$	$0.1-20$		40	20	0.1	$\lesssim 0.5$	20	
$0.03-1$	$0.05-0.1$		20	20	λ_∞	$\lesssim 0.5$	$6-12$	
$0.03-1$	0.01		20	10	$(1-2)\lambda_\infty$	$\lesssim 0.5$	6	
$1-2$	$0.05-20$		10	10	0.05	$\lesssim 0.5$	20	
$1-2$	$0.01-0.05$		10	10	λ_∞	$\lesssim 0.5$	12	
		$0.02-0.3$						$\sim(1-5)\times 10^6$
		$0.3-3$						$\sim 10^5-10^6$

TABLE SM 1. Parameters of the numerical method for various Mach, Ma, and Knudsen, Kn, numbers and rotational velocity coefficients W. Simulations of subsonic flows at $Kn = 0.01$ were performed on non-homogeneous Cartesian meshes with variable cell size

Passing Interface (MPI) communication library. In parallel simulation, the computational domain is divided into a three-dimensional array of rectangular sub-domains. Every sub-domain is a subject of computations at an individual node of a compute cluster. The number of sub-domains was ranged from 1 to 2048 depending on Ma and Kn under consideration.

SM 2. Parameters of the numerical algorithm

The set of parameters of the numerical algorithm includes the sizes of the computational domain H and L, the cell size Δ, the time step Δt, the typical number of simulated molecules in a cell of the computational domain N_{cell}, the time, which is needed to establish the quasi-steady-state flow $\Delta t \bar{N}_{est}$, the number of sampling steps $\bar{N}_{sample}$, and also some other parameters that are specific for the NTC approach to the collision sampling (Bird 1994). The time step Δt is represented in the form $\Delta t = C_{\Delta t}\tau_\infty$ where $\tau_\infty = \lambda_\infty/\sqrt{8kT_\infty/(\pi m)}$ is the mean free time between collisions of gas molecules in the free stream. The coefficient $C_{\Delta t}$ is chosen to satisfy the conditions $\Delta t \leqslant 0.5\tau_c$ and $\Delta t \leqslant 0.5\Delta/(U_c+2C_c)$ in every cell of the computational domain (Here τ_c, C_c, and U_c are the mean free time of gas molecules, their mean-square thermal velocity, and the absolute value of the gas velocity in a cell). The value of $\bar{N}_{est}$ is chosen based on the condition $U_\infty \Delta t \bar{N}_{est}/L \approx 10$. The values of other numerical parameters are listed in table SM 1.

The values of $\bar{N}_{sample}$ indicated in table SM 1 were used if only the aerodynamic and heat flux coefficients are computed. The fields of macroscopic gas parameters are determined using larger (up to ten times) number of sampling steps. In order to decrease the level of statistical scattering some computed fields of macroscopic gas parameters were smoothed by a simple linear filter. In all such cases, the smoothed fields were compared with the original non-smoothed fields in order to ensure the absence of artefacts induced by the smoothing.

A special study was conducted in order to assess the effect of all numerical parameters in transitional flow (Volkov 2007). Computational errors were estimated in simulations, where the parameters of the numerical method were varied. For values of the numerical parameters listed in table SM 1, the upper limits of computational errors in aerodynamic coefficients C_D, C_L, and C_T are found to be less than 9% for $0.01 \leqslant Kn < 0.1$ and $0.03 \leqslant Ma < 0.6$; less than 7% for $0.01 \leqslant Kn < 0.1$ and $Ma > 1$; and less than 3-5% for other conditions under consideration.

SM 3. Validation of the computer code. The drag and heat flux coefficients of a non-rotating sphere in transitional flow

In order to verify the computer code, free molecular flows over a spinning sphere were calculated numerically. The maximal difference between numerical values of coefficients C_D, C_L, C_T, and C_Q and their values calculated with the analytical solution (Appendix A) were found to be less than 1% in both sub- and supersonic flows.

In order to validate the computer code, the computed values of the drag and heat flux coefficients of a non-rotating sphere were compared with the available experimental data and their empirical fits in transitional flow. The computed values of the drag coefficient C_D are plotted in figure SM 2 as functions of the Reynolds number Re along with symbols, corresponding to experimental data by Bailey & Hiatt (1971) and values C_D^H and C_D^{MA} calculated with the semi-empirical equations proposed by Henderson (1976) and Morsi & Alexander (1972), respectively. Bold square symbols in figure SM 2(*b*) correspond to the experimental data by Zarin (1970) extrapolated to $Ma = 0.6$.

Computational results in figure SM 2(*a*–*c*) are obtained for a spinning sphere. The difference between them and corresponding values of C_D computed for a non-rotating sphere, however, is found to be less than 4%, so the effect of W on C_D is weak. The comparison of solid curves in figure SM 2(*c*) confirms this fact: Though obtained for $W = 0.1$ and $W = 1$, these curves almost coincide with each other.

The agreement between the experimental data and computational results is surprisingly good within the entire ranges of Ma and Re under consideration except one 'out-of-order' point in figure SM 2(*d*). With exception of this point, the maximal difference between C_D computed in the DSMC simulations at $\alpha_\tau = 1$ and the data by Bailey & Hiatt (1971) is less than 7%.

In continuum subsonic flow at $Ma \leqslant 0.6$, C_D^H and C_D^{MA} are close to each other. If Kn is small enough, the agreement between C_D at $\alpha_\tau = 1$ and C_D^H is also fairly good. At $Kn \approx 1$, however, the difference between C_D and C_D^H becomes large, especially in transonic flows. In the limit of free molecular flow at $Ma < 1$ and $T_s/T_\infty = 1$, values of C_D^H approach $C_D^{H(fm)} \approx 4.07/S + 0.6S$. The limit values $C_D^{H(fm)}$ are close to C_D calculated for free molecular flow with (A 9) at $\alpha_\tau = 0.9$ and $T_s/T_\infty = 1$. For instance, $C_D^{H(fm)} \approx 22.4$ at $Ma = 0.2$, while $C_D \approx 22.35$. A large discrepancy between computed C_D and C_D^H is caused by the non-monotonous behaviour of $C_D^H(Re)$ at small Reynolds numbers as it is clearly seen in figure SM 2(*a*–*c*). The non-monotonous dependence $C_D^H(Re)$ appears to be unjustified from the physical point of view, therefore, the discrepancy between C_D^H and computed C_D is attributed to a defect of the equation proposed by Henderson (1976).

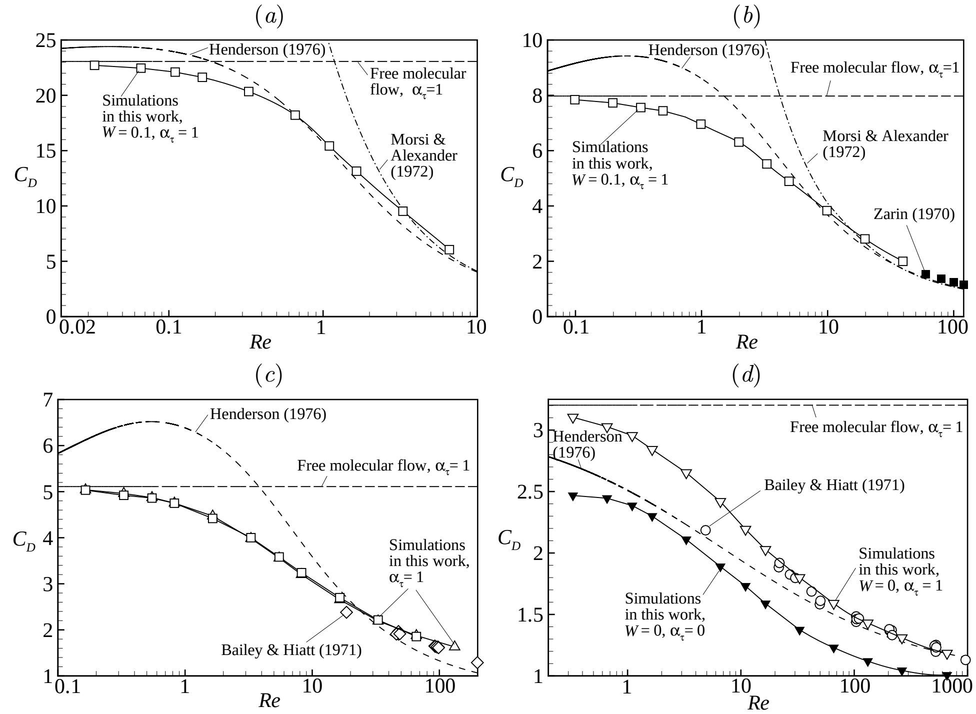

FIGURE SM 2. Drag coefficient C_D versus Reynolds number Re at $Ma = 0.2$ (a), 0.6 (b), 1 (c) and 2 (d). – . – . –, Morsi & Alexander (1972); – – –, Henderson (1976) at $T_s/T_\infty = 1$ and $\gamma = 5/3$; — — —, free molecular flow, (A 9) at $T_s/T_\infty = 1$ and $\alpha_\tau = 1$; ■, extrapolation of the experimental data by Zarin (1970) at $Ma = 0.6$; ◇, Bailey & Hiatt (1971), $1.003 \leqslant Ma \leqslant 1.19$; ○, Bailey & Hiatt (1971), $1.9 \leqslant Ma \leqslant 2.2$; other symbols and solid curves, simulations in the present work at $T_s/T_\infty = 1$ and $\Theta = 90°$: □, $W = 0.1$, $\alpha_\tau = 1$; △, $W = 1$, $\alpha_\tau = 1$; ▽, $W = 0$, $\alpha_\tau = 1$; ▼, $W = 0$, $\alpha_\tau = 0$. The data are partly taken from (Volkov 2009).

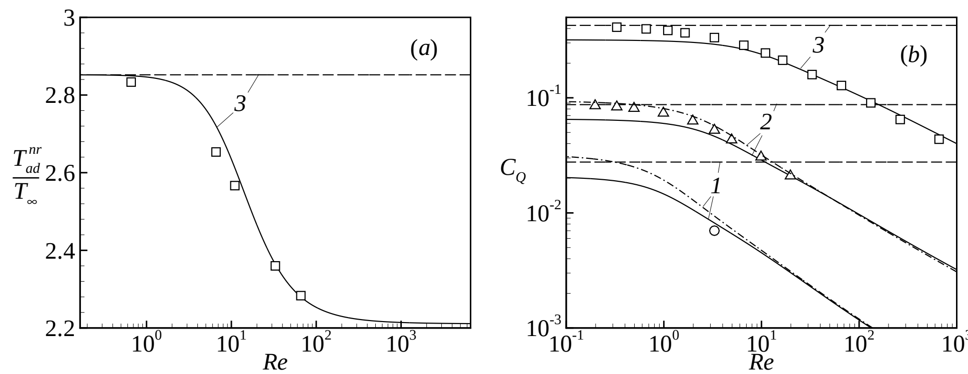

FIGURE SM 3. Dimensionless adiabatic temperature T_{ad}^{nr}/T_∞ (a) and heat flux coefficient C_Q (b) of a non-rotating sphere versus Reynolds number Re. ——, Koshmarov & Svirshevskii (1972); – . – . –, Kavanau (1955) with the adiabatic temperature calculated with the equation proposed by Koshmarov & Svirshevskii (1972); — — —, free molecular flow at $W = 0$ and $\alpha_\tau = 1$, (A 17)–(A 20); symbols, simulations in the present work at $T_s/T_\infty = 1$ and $\alpha_\tau = 1$. Curves 1 and ○, $Ma = 0.2$; curves 2 and △, $Ma = 0.6$; curves 3 and □, $Ma = 2$.

The computed adiabatic temperature of a non-rotating sphere T_{ad}^{nr} agrees fairly well with an empirical equation proposed by Koshmarov & Svirshevskii (1972) (Figure SM 3(a)). In figure SM 3(b), the computed values of C_Q for $T_s/T_\infty = 1$ and $\alpha_\tau = 1$ are compared with the values of the heat flux coefficient C_Q^K and C_Q^{KS} that are obtained based on approximate equations proposed by Kavanau (1955) and Koshmarov & Svirshevskii (1972), respectively. In calculations of both C_Q^K and C_Q^{KS}, the adiabatic temperature T_{ad}^{nr} is estimated from an equation obtained by Koshmarov & Svirshevskii (1972). The dashed curves correspond to the values of the heat flux coefficient C_Q^{fm} calculated for free molecular flow with (A 17)–(A 20) at $W = 0$ and $\alpha_\tau = 1$. For relatively large Re, the values of C_Q are in good agreement with C_Q^{KS}. As Re decreases, the computed values of C_Q approach C_Q^{fm}, while C_Q^{KS} approaches $(3/4)C_Q^{fm}$. This is the reason for the difference between C_Q and C_Q^{KS} at small Re. In subsonic transitional flows, C_Q^K fits the computed values of C_Q better than C_Q^{KS}. At larger Re, C_Q^K and C_Q^{KS} almost coincide with each other.

Experimental values of C_Q for conditions under consideration are not shown in figure SM 3. They can be re-calculated based on experimental values of the Nusselt number and the adiabatic temperature, see Kavanau (1955) and Koshmarov & Svirshevskii (1972), and references wherein.

Thus, the computed values of C_D and C_Q for a non-rotating sphere are in a fairly good agreement with the available experimental data and in partial agreement with the semi-empirical approximations. At $Kn \sim 0.1 - 0.01$, the differences between the computed values of C_D and C_Q and corresponding values found with empirical equations by Henderson (1976) and Koshmarov & Svirshevskii (1972) are small. The differences, however, tend to be larger at $Kn \sim 1$. It is likely that the last circumstance is the consequence of defects of these semi-empirical fits at large Knudsen numbers that correspond to nearly free molecular flows.

SM 4. Derivation of empirical approximations of the aerodynamic and heat flux coefficients of a spinning sphere at $T_s/T_\infty = 1$

The functions C_a^* in (B 1), (B 3), (B 8), and (B 11) are derived to fit the computed values of corresponding coefficients at $Kn^* = 0.1$ for $W = 0.03$, 0.1, 0.3 and 1. At constant W, the functions $C_a^*(Ma)$ are shown in figure 10 by dashed curves.

The derivation of functions β_a and K_a includes two stages. At the first stage, values of these functions are computed in a discrete set of points (Ma_i, W_j) from a condition of the best agreement between values obtained in simulations and predicted by (4.1). At the second stage, computed values of $\beta_a(Ma_i, W_j)$ and $K_a(Ma_i, W_j)$ are further approximated by simple empirical correlations. In derivation of these correlations, a partial similarity of dependencies of the coefficients on Ma and W in free molecular and transitional flows is exploited, where it is possible.

Equations (4.1)–(4.4), (A 8)–(A 9), (A 12)–(A 15), (A 17)–(A 21), and (B 1)–(B 15) can be used for calculation of C_D, C_L, C_T, and C_Q in subsonic flows at $Ma \geqslant 0.03$ and $Kn \geqslant 0.05$ and in supersonic flows at $Ma \leqslant 2$ and $Kn \geqslant 0.01$ for $0.02 \leqslant W \leqslant 1$, and $T_s/T_\infty = 1$. The maximal and mean-square relative discrepancies between the approximate equations and the data obtained in the DSMC simulations within these ranges of governing parameters are shown in table SM 2. The simulations where the temperature ratio is varied (Figure 17) show that, in the first approximation, coefficients C_D, C_L, and C_T can be assumed to be independent of T_s/T_∞ if $|T_s/T_\infty - 1| \lesssim 0.2$.

Coefficient, C_a	C_D	C_L	C_T	C_Q
Reference value, C_a^{ref}	C_D^s	4/3	C_T^s	C_Q^s
Maximal value of $\Delta(C_a)$, %	8.8	6.7	8.8	14.8
Mean-square value of $\Delta(C_a)$, %	2.6	3.5	3.4	5.6

Table SM 2. Maximal and mean-square discrepancies $\Delta(C_a) = |(C_a^s - C_a^a)/C_a^{ref}| \times 100\%$ between values of coefficients C_a^s obtained in the DSMC simulation and their values C_a^a predicted by (4.1)–(4.4), (A 8)–(A 9), (A 12)–(A 15), (A 17)–(A 21), and (B 1)–(B 15) at $0.05 \leqslant Kn \leqslant 20$ in subsonic flows with $0.03 \leqslant Ma \leqslant 1$ and at $0.01 \leqslant Kn \leqslant 20$ in supersonic flows with $1 \leqslant Ma \leqslant 2$, when $0.03 \leqslant W \leqslant 1$, $T_s/T_\infty = 1$, $\Theta = 90°$, and $\alpha_\tau = 1$

REFERENCES

Bailey, A.B. & Hiatt, J. 1971 Free-flight measurements of sphere drag at subsonic, transonic, supersonic, and hypersonic speeds for continuum, transition, and near-free-molecular flow conditions. *Tech. Rep.* AEDC-TR-70-291. Arnold Engineering Development Center report.

Bird, G.A. 1994 *Molecular gas dynamics and the direct simulation of gas flows*. Clarendon Press, Oxford.

Cercignani, C. 2000 *Rarefied gas dynamics: From basic concepts to actual calculations*. Cambridge University Press, Cambridge.

Henderson, C.B. 1976 Drag coefficients of spheres in continuum and rarefied flows. *AIAA J.* **14**, 707–708.

Ivanov, M.S. & Gimelshein, S.F. 1998 Computational hypersonic rarefied flows. *Annu. Rev. Fluid Mech.* **30**, 469–505.

Ivanov, M.S. & Rogasinsky, S.V. 1988 Analysis of numerical techniques of the direct simulation Monte Carlo method in the rarefied gas dynamics. *Sov. J. Numer. Anal. Math. Model.* **2**, 453–465, translated from Zhurnal Vychislitelnoi Matematiki i Matematicheskoi Fizuiki, 1988, **28**, 1058-1070.

Kavanau, L.L. 1955 Heat transfer from spheres to a rarefied gas in subsonic flow. *Trans. ASME* **77**, 617–623.

Koshmarov, Y.A. & Svirshevskii, S.B. 1972 Heat transfer from a sphere in the intermediate dynamics region of a rarefied gas. *Fluid dynamics* **7**, 343–346, translated from Izvestiya Akademii Nauk SSSR, Mekhanika Zhidkosti i Gaza, 1972, No. 2, 170-172.

Matsumoto, M. & Nishimura, T. 1998 Mersenne twister: A 623-dimensionally equidistributed uniform pseudo-random number generator. *ACM Transactions on Modeling and Computer Simulation* **8**, 3–30.

Morsi, S.A. & Alexander, A.J. 1972 An investigation of particle trajectories in two-phase flow systems. *J. Fluid Mech.* **55**, 193–208.

Nanbu, K. 1980 Direct simulation scheme derived from the Boltzmann equation. I. Monocomponent gases. *J. Phys. Soc. Japan* **49**, 2042–2049.

Volkov, A.N. 2007 The aerodynamic and heat properties of a spinning spherical particle in transitional flow. In *6th International Conference on Multiphase Flow, Leipzig, Germany, July 9-13, 2007* (CD-ROM Proc. ICMF 2007), paper S2_Mon_C_6.

Volkov, A.N. 2009 Aerodynamic coefficients of a spinning sphere in a rarefied-gas flow. *Fluid dynamics* **44**, 141–157, translated from Izvestiya Rossiiskoi Akademii Nauk, Mekhanika Zhidkosti i Gaza, 2009, **44**, 167–187.

Wagner, W. 1992 A convergence proof for Bird's direct simulation Monte Carlo method for the Boltzmann equation. *J. Stat. Phys.* **66**, 1011–1044.

Zarin, N.A. 1970 Measurment of non-continuum and turbulence effects on subsonic sphere drag. *Tech. Rep.* CR-1585. NASA Report.